Characterization of a Mechanism-Based Inhibitor of NAD(P)H:Quinone Oxidoreductase 1 by Biochemical, X-ray Crystallographic, and Mass Spectrometric Approaches†

Shannon L. Winski,‡ Margarita Faig,§ Mario A. Bianchet,§ David Siegel,‡ Elizabeth Swann,‖ Kim Fung,‡ Mark W. Duncan,‡ Christopher J. Moody,‖ L. Mario Amzel,§ and David Ross*,‡

Department of Pharmaceutical Sciences, School of Pharmacy, University of Colorado Health Sciences Center, Denver, Colorado 80262, School of Chemistry, University of Exeter, Exeter, U.K., and Department of Biophysics and Biophysical Chemistry, Johns Hopkins Medical School, Baltimore, Maryland 21205

Received June 25, 2001; Revised Manuscript Received October 9, 2001

ABSTRACT: We report the characterization of 5-methoxy-1,2-dimethyl-3-[(4-nitrophenoxy)methyl]indole-4,7-dione (ES936) as a mechanism-based inhibitor of NQO1. Inactivation of NQO1 by ES936 was time- and concentration-dependent and required the presence of a pyridine nucleotide cofactor consistent with a need for metabolic activation. That ES936 was an efficient inhibitor was demonstrated in these studies by the low partition ratio (1.40 ± 0.03). The orientation of ES936 in the active site of NQO1 was examined by X-ray crystallography and found to be opposite to that observed for other indolequinones acting as substrates. ES936 was oriented in such a manner that, after enzymatic reduction and loss of a nitrophenol leaving group, a reactive iminium species was located in close proximity to nucleophilic His 162 and Tyr 127 and Tyr 129 residues in the active site. To determine if ES936 was covalently modifying NQO1, ES936-treated protein was analyzed by electrospray ionization liquid chromatography/mass spectrometry (ESI-LC/MS). The control NQO1 protein had a mass of 30864 ± 6 Da ($n = 20$, theoretical, 30868.6 Da) which increased by 217 Da after ES936 treatment (31081 ± 7 Da, $n = 20$) in the presence of NADH. The shift in mass was consistent with adduction of NQO1 by the reactive iminium derived from ES936 (M + 218 Da). Chymotryptic digestion of the protein followed by LC/MS analysis located a tetrapeptide spanning amino acids 126−129 which was adducted with the reactive iminium species derived from ES936. LC/MS/MS analysis of the peptide fragment confirmed adduction of either Tyr 127 or Tyr 129 residues. This work demonstrates that ES936 is a potent mechanism-based inhibitor of NQO1 and may be a useful tool in defining the role of NQO1 in cellular systems and in vivo.

NAD(P)H:quinone oxidoreductase (NQO1,[1] DT-diaphorase, EC 1.6.99.2) is generally considered to be a deactivation enzyme because of its ability to detoxify reactive quinones and quinone imines to yield less reactive and less toxic hydroquinones (*1*−*3*). NQO1 also plays a role as an antioxidant enzyme and generates antioxidant forms of ubiquinone (*4*, *5*) and α-tocopherol after free radical attack (*6*). As a result of its protective effects, NQO1 has been proposed to function as a chemopreventive enzyme (*7*−*9*). NQO1, however, may also catalyze bioactivation of antitumor quinones, and this is currently under consideration as a therapeutic strategy (*10*−*12*). Using NQO1 as the principal target to design chemotherapeutic agents is of significant interest because it is expressed at high levels throughout many human solid tumors such as lung, colon, ovarian, eye, and breast tumors (*13*−*16*).

The role of NQO1 in biochemical systems has traditionally been determined by the use of the competitive inhibitor dicoumarol, which binds reversibly to the pyridine nucleotide binding site on NQO1 and is competitive against pyridine nucleotide (*17*, *18*). Dicoumarol has been used as a component of the standard activity assay for NQO1 for many years (*1*), but it is not selective and can inhibit many enzymes in addition to NQO1 (*10*). Dicoumarol is also extensively protein bound (*19*), which can complicate its use in cellular systems. Furthermore, the effective concentration of dicoumarol that is required to inhibit NQO1 depends on the efficiency of the second substrate or electron acceptor because of the competitive nature of dicoumarol inhibition and the ping-pong kinetic mechanism of NQO1 (*20*). Flavone-8-acetic acid and 5,6-dimethylxanthenone-4-acetic acid have also been recently described as inhibitors of NQO1 (*21*), but these compounds also have significant shortcomings

† This work was supported by NIH Grant R01 CA51210, NRSA Grant CA79446, and The Cancer Research Campaign.

* To whom correspondence should be addressed. Telephone: 303-315-6077. Fax: 303-315-0274. E-mail: David.Ross@uchsc.edu.

‡ University of Colorado Health Sciences Center.

§ Johns Hopkins Medical School.

‖ University of Exeter.

[1] Abbreviations: NQO1, NAD(P)H:quinone oxidoreductase 1; DQ, 2,3,5,6-tetramethyl-1,4-benzoquinone; RH1, 2,5-diaziridinyl-3-hydroxy-6-methyl-1,4-benzoquinone; CB, Cibacron Blue 3GA; DCPIP, 2,6-dichlorophenolindophenol; EO9, 3-[5-aziridinyl-3-(hydroxymethyl)-1-methyl-4,7-dioxoindol-2-yl]prop-2-enol; MeDZQ, 2,5-diaziridinyl-3,6-dimethyl-1,4-benzoquinone; ARH019, 3-(hydroxymethyl)-5-(2-methylaziridiridin-1-yl)-1-methyl-2-phenylindole-4,7-dione; hNQO1, human NQO1; rNQO1, rat NQO1; mNQO1, mouse NQO1; ESI-LC/MS, electrospray ionization liquid chromatography/mass spectrometry.

10.1021/bi011324i CCC: $20.00
Published on Web 11/20/2001

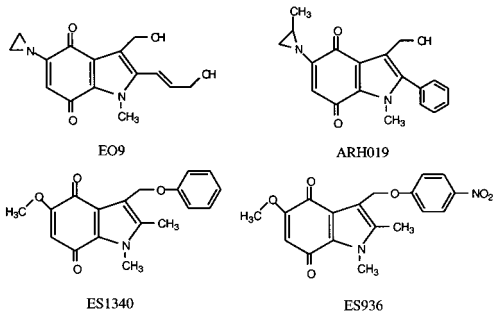

FIGURE 1: Structures of indolequinones.

such as their lack of specificity, high concentrations required for inhibition and a competitive mechanism of action.

In an attempt to develop more efficient substrates for NQO1, a large series of indolequinones have been examined (*22*−*26*). In addition to characterizing efficient substrates for NQO1 in the indolequinone series such as EO9 and ARH019 (Figure 1), during these studies several compounds were observed to be inhibitors of NQO1 (*24*−*26*) such as 5-methoxy-1,2-dimethyl-3-[(4-nitrophenoxy)methyl]indole-4,7-dione (ES936, Figure 1). Considerable work on the structure of NQO1 using X-ray crystallography has been described recently. The X-ray crystal structures of NQO1 reported previously have shed light on the enzyme mechanism (*27*, *28*) and the catalytic differences among species (*28*−*30*). Most recently, we have reported the resolved structures of several antitumor quinones, including the indolequinones ARH019 and EO9, complexed in the active site of human NQO1 (*31*). These structures have proved extremely valuable in the characterization of the mode of inhibition of NQO1 by the indolequinone inhibitor ES936. In this paper, we report the characterization of ES936 as a potent mechanism-based inactivator of NQO1 using a combination of biochemical, X-ray, and mass spectrometric techniques.

MATERIALS AND METHODS

Materials. Expression of human recombinant NQO1 in *Escherichia coli* and its subsequent purification were carried out using methods described previously (*32*). The synthesis of ES1340 and ES936 has been described by Moody and co-workers (*25*, *33*).

NQO1 Activity Assay. The activity of purified recombinant NQO1 was measured by the rate of reduction of 2,6-dichlorophenolindophenol (DCPIP) as described previously (*8*).

Inactivation Kinetics of ES936. Inactivation of NQO1 by ES936 was very rapid; therefore, determination of time and concentration dependence was carried out at 4 °C. NQO1 (4 μg/mL) was preincubated for 15 min with NADH (100 μM) in 50 mM potassium phosphate buffer, pH = 7.4, containing 2 mg/mL Tween 20 at 4 °C. For kinetic analysis 0.5 mL of enzyme solution (65 pmol) was added to 0.5 mL of ice-cold 50 mM potassium phosphate buffer, pH 7.4, containing ES936 (0.125−2 μM final concentration). At predetermined time points, aliquots (10 μL) were removed and diluted 100-fold with DCPIP reaction buffer (50 mM potassium phosphate buffer, pH 7.4, containing 1 mg/mL bovine serum albumin and 0.2 mM NADH). Following addition of DCPIP (40 μM), NQO1 activity was determined spectrophotometrically at 600 nm. Statistical analysis was performed using SigmaStat software and linear regression of the Kitz and Wilson plot. The standard error of the linear regression analysis was propagated algebraically throughout the calculations of K_I and k_{inact} to obtain an estimate of the standard error of these determinations. To determine the partition ratio, NQO1 (65 nM) was incubated with ES936 (0−200 nM) and allowed to react to completion. Aliquots of this reaction mixture (50 μL) were removed and diluted with 200 μL of ice-cold 50 mM potassium phosphate buffer, pH 7.4, containing 0.25 M sucrose. NQO1 activity was measured by the rate of reduction of DCPIP as described above. Partition ratios were calculated from linear plots of percent activity remaining versus molar ratio of ES936 to NQO1.

NADH Dependence of ES936 Inhibition. The requirement of NADH for inactivation of NQO1 by ES936 was assayed essentially as described above. Briefly, NQO1 (668 pmol) was incubated in the presence and absence of NADH (500 nmol) in 10 mL of 50 mM potassium phosphate, pH 7.4, containing Tween 20 (2 mg/mL) and ES936 (1.3 nmol). Control reactions were performed in the absence of either ES936 or NADH. After 5 min an aliquot was removed and assayed for NQO1 activity using DCPIP reduction as described above.

X-ray Crystallography. (A) Crystallization and Data Collection. Human NQO1 crystals, grown as previously described (*28*), belong to the triclinic space group *P*1 with cell dimensions of $a = 55.7$ Å, $b = 57.0$ Å, $c = 97.4$ Å, $\alpha = 76.7°$, $\beta = 77.0°$, and $\gamma = 86.0°$. Crystals contain two physiological dimers in the asymmetric unit. Due to the low solubility of indolequinones in the mother liquor solution, the complexes were obtained by soaking native crystals overnight in indolequinone-saturated mother liquor. Diffraction data for ES936 were collected at the National Synchrotron Light Source of the Brookhaven National Laboratory at beam line X25 with a Brandeis charge-coupled device (CCD) detector using a wavelength of 1.1 Å. Diffraction data for the ES1340 complex were collected with a rotating anode (Cu Kα) source using a Raxis IV$^+$ detector. Data for both complexes were collected at 100 K after flash freezing the crystal by immersion in liquid nitrogen in unmodified mother liquor. All data were reduced with the software package HKL (*34*).

(B) Structure Determination and Refinement. Initial structures were modeled using the coordinates of the apo (with FAD)-hNQO1 structure (PDB accession code 1D4A). For each complex the positions of the four monomers were refined independently as rigid bodies. Difference Fourier electron density maps calculated after convergence showed density for the compounds in the four active sites. Drug models were built using parameters and topologies derived from related compounds, including *p*-benzoquinones, reported in the Cambridge Structural Database (*35*) and solved. The structural models of the complexes were refined with the program CNS (*36*). A torsional molecular dynamics refinement, either at constant temperature (2000 K) or as a slow cooling annealing, was followed by energy minimization, restrained *B* factor refinement, and manual rebuilding in sigmaA weighted maps using the program O (*37*). The atomic coordinates of the hNQO1−ES1340 complex (code 1KBO) and hNQO1−ES936 (code 1KBQ) have been

deposited in the Protein Data Bank. Figures were drawn with the programs MOLSCRIPT (*38*), BOBSCRIPT (*39*), and RASTER3D (*40*). Structure quality was assessed with the program PROCHECK, part of the suite of programs CCP4. Molecular surfaces were drawn with the program GRASP (*41*). Solvent-accessible surface areas (ASA) were calculated with the program NACCESS (*42*).

Sample Preparation for Mass Spectrometry (MS). ES936-treated samples of human recombinant NQO1 protein for MS analysis were prepared by inactivation of NQO1 with a 3-fold molar excess of ES936 (dissolved in DMSO) in 25 mM potassium phosphate buffer, pH 7.4. Control samples were treated with an equivalent volume of DMSO in the same buffer. Enzyme activity was monitored to ensure that the protein was more than 95% inhibited. The protein sample was then concentrated (Amicon, Millipore) and rinsed in doubly distilled H_2O followed by rinsing in 1% trifluoroacetic acid (TFA). The TFA treatment causes dissociation of the FAD moieties from the protein which interfere in the MS analysis.

ESI Mass Spectrometry. The masses of control and ES936-treated NQO1 were determined by ESI-LC/MS on an ion trap mass spectrometer (LCQDeca, Finnigan, San Jose, CA) following reverse-phase chromatography using POROS R1 resin (Perseptive Biosystems, Framingham, MA). The intact molecular mass of proteins was obtained by deconvolution of the multiply charged ion envelope evident in each spectrum. Subsequently, control and ES936-treated NQO1 samples were digested with chymotrypsin (37 °C, overnight) and analyzed by electrospray tandem mass spectrometery (ESI-LC/MS/MS). Peptides were first separated by reverse-phase chromatography using a capillary column (150 μm i.d.) packed with POROS R2 resin (Perseptive Biosystems, Framingham, MA). Peptides were eluted (flow rate 5 μL/min) over 60 min with an increasing linear gradient of acetonitrile/0.05% TFA (0−100%). The peptide of interest was fragmented to produce MS/MS product ion spectra, and the sequence and sites of modification were determined by de novo sequencing.

RESULTS

Kinetic Analysis of ES936 Inactivation. The inactivation of NQO1 by ES936 was very rapid, and consequently, the time and concentration dependence of the inhibition kinetics were determined at 4 °C rather than at room temperature. The rate of inactivation was proportional to concentration at low concentrations of ES936 (Figure 2) and independent at higher concentration, demonstrating saturation kinetics. K_I and k_{inact} were determined from Kitz and Wilson plots as described (*43*), and the values estimated for ES936 were $K_I = 0.45 \pm 0.07$ μM and $k_{inact} = 0.78 \pm 0.12$ min^{-1}. A more important descriptive term for mechanism-based inactivators is the partition ratio. It is used to describe the effectiveness of an inhibitor and relates to the number of inhibitor molecules released from the active site in relation to the number which remain to inactivate the enzyme (*43*). The partition ratio for ES936 was 1.40 ± 0.03 (Figure 3), indicating that ES936 is an efficient inactivator of NQO1. An important criterion for mechanism-based inactivation is the requirement for a catalytic step to occur prior to enzyme inactivation. Incubation of ES936 with NADH and NQO1 resulted in greater than 99% inhibition of enzyme activity whereas in the absence of the cofactor NADH, no loss of enzyme activity was observed (Figure 4).

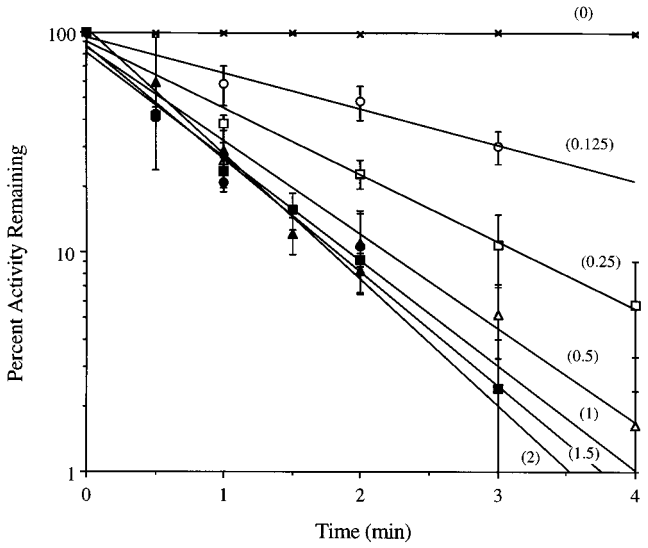

FIGURE 2: Time- and concentration-dependent inhibition of NQO1 by ES936. Inactivation kinetics were performed as described in Materials and Methods. Concentrations of ES936 (μM) are shown in parentheses adjacent to the appropriate best fit line. Data represent mean ± standard deviation of three independent determinations.

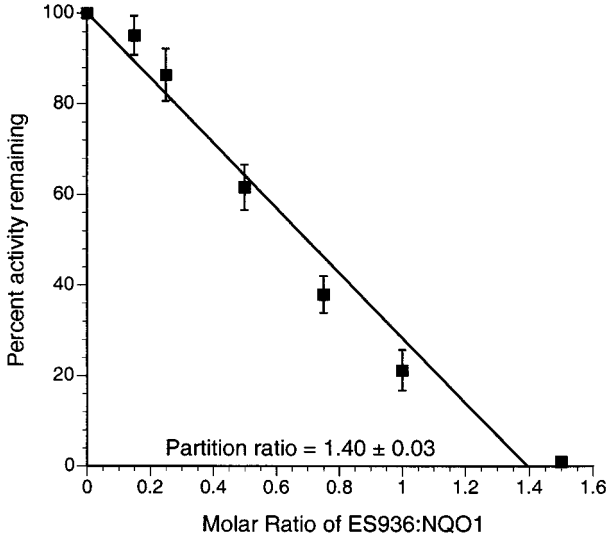

FIGURE 3: Inactivation of NQO1 by ES936: calculation of partition ratio. NQO1 was preincubated in the presence of NADH and Tween 20 (enzyme activator). ES936 was added and allowed to react to completion (15 min). NQO1 activity was measured, and partition ratio was calculated from linear plots of percent activity remaining versus molar ratio of ES936 to NQO1. Data represent mean ± standard deviation of four independent determinations.

Crystal Structure Determination of the hNQO1−ES936 Complex. The crystal structure of the complex of hNQO1 with ES936 was determined and refined to an *R*-value of 20.1%, with excellent stereochemistry (Table 1). The structure had four copies of the hNQO1−drug complex (four monomers in the asymmetric unit). Final $2F_o - F_c$ maps show excellent density for most portions of the polypeptide chains and for the four copies of the bound compounds (Figure 5). NQO1 is a physiological homodimer made of two interlocked monomers of 273 residues related by a noncrystallographic 2-fold axis of symmetry. Each NQO1

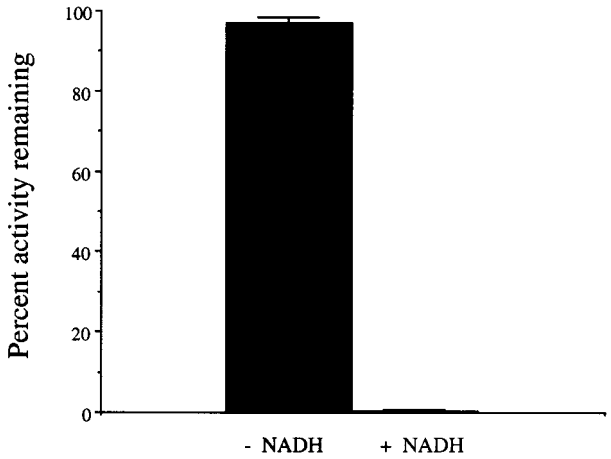

FIGURE 4: NADH-dependent inactivation of NQO1 by ES936. The effect of ES936 on NQO1 activity in the presence and absence of NADH was determined as described in Materials and Methods. Percentage activity was determined relative to control incubations of NQO1 in buffer. Data represent mean ± standard error of the mean of four independent determinations.

Table 1: Summary of the Crystallographic Analysis

substrate	ES1340	ES936
resolution	2.3	1.8
unique reflections	47881	103269
multiplicity	2.7	3.4
completeness (%)	96.5 (94.3)	98 (85)
R_{sym}[a] × 100	9.8	9.6
no. of reflections used	37347 (74%)	99339 (90%)
no. of model atoms	9109	9494
no. of ligand atoms	304	316
no. of solvent atoms	165	514
R_{cryst}/R_{free}	20.4/28.6	21.5/25.7
intensity cutoff	2.0	0.0
RMS/RMS angles	0.008/1.3	0.008/1.39
protein temp factors (Å^2)	32.4	24.7
ligand temp factors (Å^2)	40.1	31.0
solvent temp factors (Å^2)	33.1	26.9
PDB ID code	1KBO	1KBQ

[a] $R_{sym} = \sum_h\sum_{fj}|I_{fj} - \langle I_h\rangle|/\sum_h\sum_{fj}|I_{hj}|$, where h represents a unique reflection and j means symmetry equivalent indices. I is the observed intensity, and $\langle I\rangle$ is the mean value of I.

monomer is composed of two domains: a large catalytic domain (residues 1−220) and a small C-terminal domain (residues 221−273). The catalytic domain has an α/β fold with flavodoxin topology. Alignments of the apo (with FAD) human dimer (PDB accession code 1D4A) with a dimer of each complex yield RMS deviations for the 544 α-carbon atoms of 0.31 Å.

The structural changes associated with substrate binding occur at one side of the binding pocket (Figure 6), involving only a few residues located above isoallozaxine rings A and B. Tyr 129′,[2] and Phe 233′ show the largest displacements with respect to the apo (with FAD) hNQO1 structures reported earlier (*28*).

ES936 is bound to the two equivalent catalytic sites in each dimer. It binds, interacting with the bound FAD and with residues of both monomers. The plane of ES936 stacks

[2] When referring to the catalytic site, secondary structure elements and residues from individual monomers will be primed ′or unprimed. As the two monomers are equivalent, primes will be used only when distinction is needed.

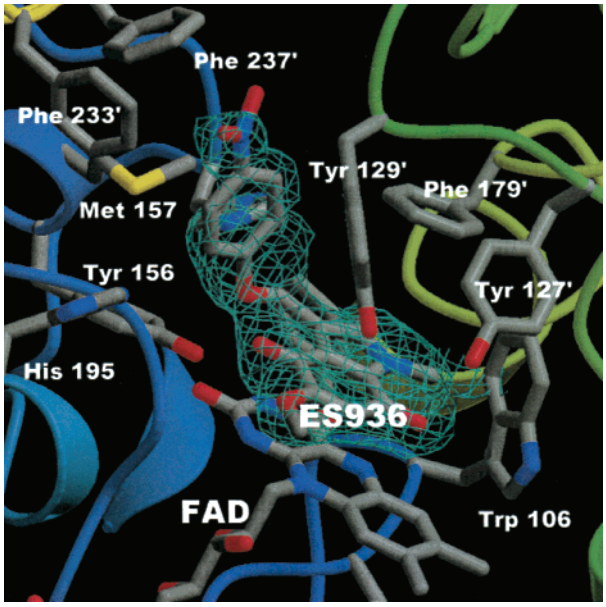

FIGURE 5: $2F_o - F_c$ electronic density map of the bound ES936. Residues of the active site, FAD, and substrate are represented in a stick model and the rest of the structure as a secondary structure cartoon. The two monomers that form the active site have distinct colors (green and light blue). The atoms are colored: red, oxygen atoms; green, sulfur atoms; blue, nitrogen atoms; and gray, carbon atoms.

parallel to the isoallozaxine ring of the FAD that forms one of the walls of the catalytic pocket. The indole ring, 1- and 2-methyl, and the bulky group at the indole 3-position are placed deeper in the catalytic site (Figure 6). One side of the latter group lies against Met 155, His 162, and Met 132′, and the other stacks with the ring of Tyr 129′. The 4,7-dione ring points out of the pocket with its 5-methoxy stacking against the glycines (150 and 151) of loop L6. The indole-1-methyl stacks against the side chain of Trp 106 and the indole-2-methyl in the pocket defined by Phe 107, Trp 106, Phe 179′, and the main chain of Ser 176′. The indolyl-1-nitrogen is the closest atom to the hydrogen at N5 of the reduced FAD (3.6 Å). Enzyme−inhibitor interactions are mostly hydrophobic contacts, with only one hydrogen bond between the indolequinone O7 and Tyr 127′. The orientation of ES936 in the active site demonstrates that, after reduction and loss of *p*-nitrophenol, a reactive iminium species will be generated in close proximity to both histidine (162) and tyrosine residues (127 and 129) in the active site of hNQO1.

Crystal Structure Determination of the hNQO1−ES1340 Complex. ES1340 (Figure 1) is an analogue of ES936 without the *p*-nitro group and therefore does not possess as good a leaving group. As a result, ES1340 is not an inhibitor of NQO1 and is actually a substrate, albeit an inefficient one (Beall and Moody, unpublished data). The compound was examined to test the hypothesis that the 4-nitro group might be critical in alignment of the indolequinone ES936 in the active site of hNQO1. In all aspects binding of ES1340 as demonstrated by the crystal structure of the hNQO1−ES1340 complex (Figure 7) was very similar to that of ES936. In the case of ES936, however (Figure 5), the loop L9′ (residues 231−237) of the C-terminal domain moves, opening the NAD adenosine site as in the NAD^+−rNQO1 DQ/CB−rNQO1 complexes to accommodate an additional nitro group. This group has contacts with Phe 233′, Phe 237′, and the

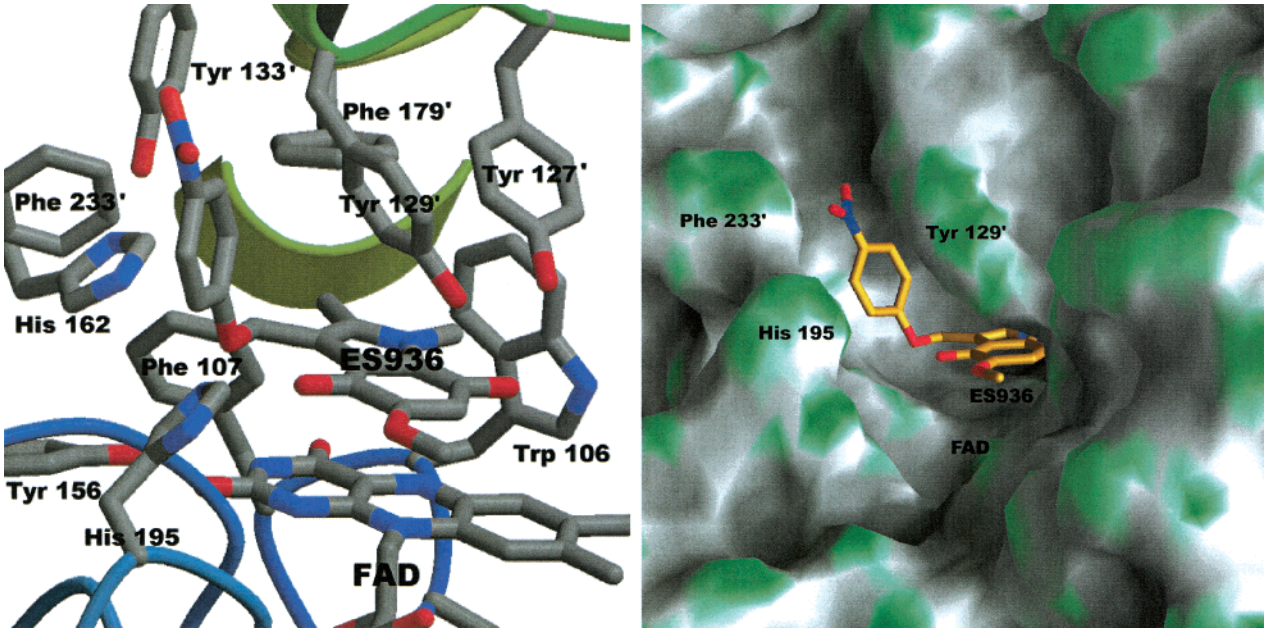

FIGURE 6: (A, left) ES936 bound to the active site of hNQO1. Residues of the active site, FAD, and substrate are represented in a stick model and the rest of the structure as a secondary structure cartoon. The two monomers that form the active site have distinct colors (green and light blue). The atoms are colored with the same color scheme as in Figure 5. (B, right) Molecular surface of the hNQO1 active site region with the substrate ES936 represented as a stick model. The green/gray coloring of the surface represents the local concave (gray) or convex (green) nature of the surface. The same coloring scheme applies as described in Figure 5 with the exception of the ES936 carbon atoms that were colored in gold.

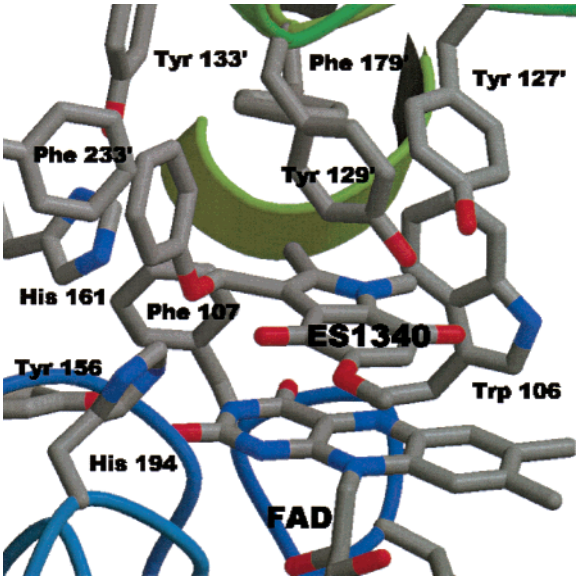

FIGURE 7: ES1340 bound to the active site of hNQO1. Residues of the active site, FAD, and substrate are represented in a stick model and the rest of the structure as a secondary structure cartoon. The color scheme is the same as in Figure 5.

main chain carboxy of Tyr 129 (3.2 Å). Alignments of the apo (with FAD) human dimer (PDB accession code 1D4A) with a dimer of the complex of ES1340 yielded RMS deviations for the 544 α-carbon atoms of 0.26 Å. Common atoms of both ES936 and ES1340 occupy the same position in the active site (RMS of 0.1 Å for 22 common atoms). The data indicate that the *p*-nitro group is not critical to orientation of ES936 in the active site of hNQO1.

MS Analysis. The molecular mass of intact NQO1 was determined to be 30864 ± 6 Da ($n = 20$) using ESI-LC/MS (cf. 30868.6 Da, the calculated average mass of protonated NQO1). After incubation of NQO1 with NADH and ES936, the molecular mass of the protein increased to 31081 ± 7 Da ($n = 20$). The mass difference between the two species (217 Da) was consistent with the mass of the proposed adduct, which should result in an increase in mass of 218 Da.

To determine the site of adduction, control and ES936-treated NQO1 proteins were digested with chymotrypsin and the resulting peptides analyzed by LC/MS/MS. Figure 8 shows a peptide mass corresponding to (MH^+) of m/z = 734.6 Da eluting at 28−30 min that was detected in the digest of the ES936-treated protein. This peptide was not detected when the control protein was analyzed. This peptide was subsequently fragmented to produce an MS/MS spectrum (Figure 9). Analysis of the MS/MS spectrum indicates that the sequence of this peptide was AYTY and corresponded to residues 126−129 of the NQO1 protein. The MS/MS spectrum also revealed the existence of two coeluting modified peptides. Analysis of the b- and y-series ions indicated that adduction occurred on either one of the two tyrosine residues but not both.

DISCUSSION

In this paper, we describe the characterization of ES936 as a mechanism-based inhibitor of hNQO1. Biochemical analyses satisfied a number of criteria required of mechanism-based-inhibiton as described by Silverman (*43*). ES936 inhibited NQO1 in a concentration- and time-dependent manner and required the presence of cofactor and therefore substrate turnover for effective inhibition of the enzyme. The partition ratio calculated from the inhibition data is 1.4, demonstrating that ES936 is an efficient inhibitor of NQO1. Confirmation of ES936 as a mechanism-based inhibitor has been performed using both X-ray and MS analysis. The X-ray analysis demonstrated the orientation of ES936 in the active site of NQO1 and implied a close proximity of the

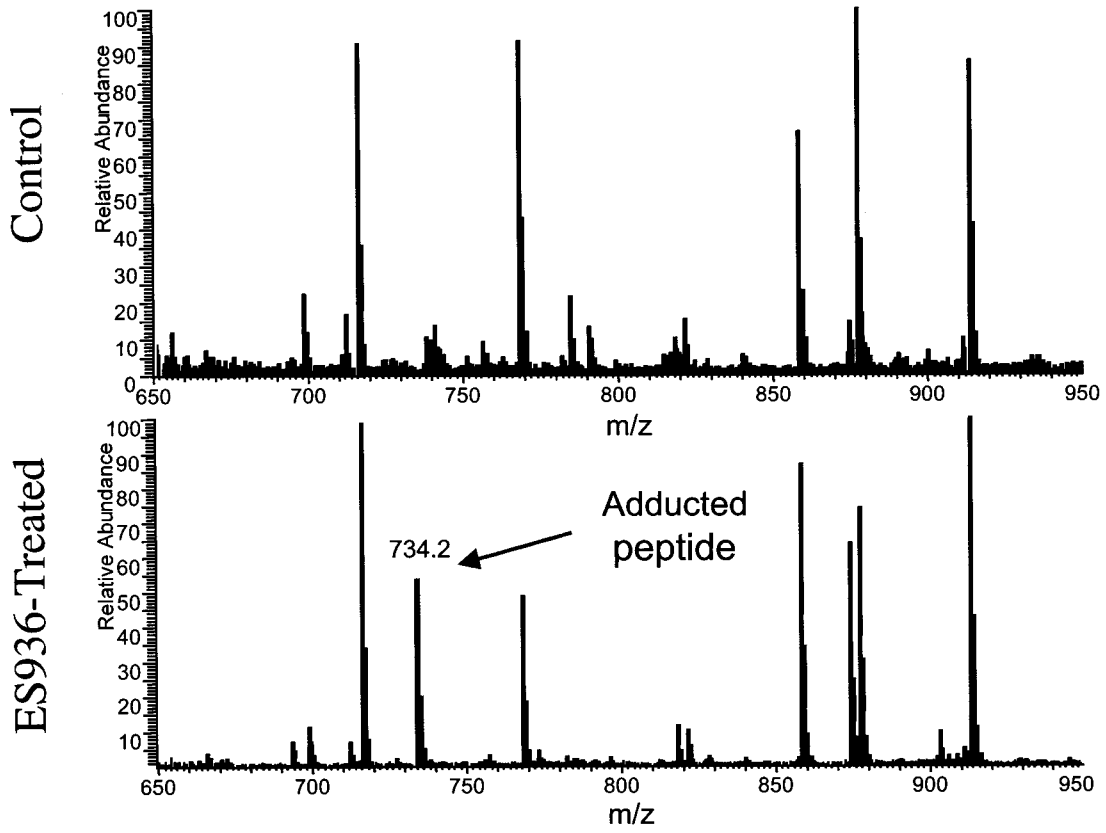

FIGURE 8: Peptide mass spectra from ESI-LC/MS analyses of chymotryptic digests of (A, top) control NQO1 (untreated) protein and (B, bottom) NQO1 protein after incubation with ES936 and NADH. The adducted peptide is shown in panel B at $m/z = 734.2$.

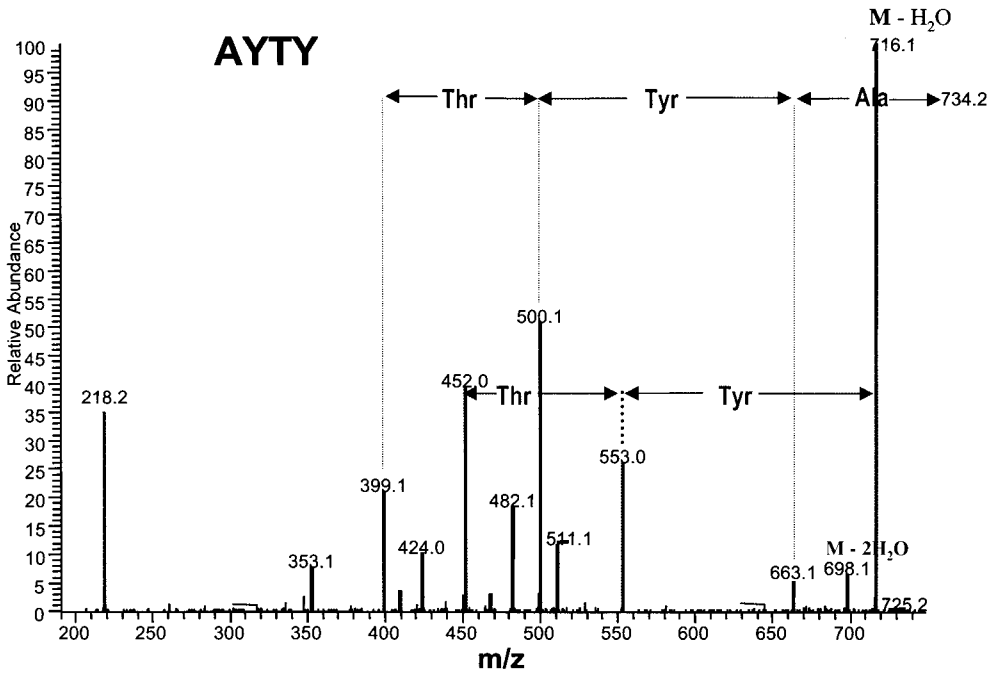

FIGURE 9: ESI-LC/MS/MS mass spectrum of the adducted peptide after incubation of NQO1 with ES936 and NADH. The product ions indicate that the site of adduction is either Tyr 127 or Tyr 129 but never both. Also detected is the adduct ion at $m/z = 218$.

ES936-derived reactive iminium species, which would be formed after enzymatic reduction and loss of the 4-nitrophenol leaving group from the indole 3-position, to nucleophilic histidine and tyrosine residues in the active site. Alkylation of NQO1 by a reactive metabolite derived from ES936 was confirmed by MALDI-TOFMS, and alkylation of tyrosine residues in the active site of NQO1 was determined by LC/MS/MS after chymotryptic digestion of the adducted protein.

The results of the MS analysis confirmed adduction of NQO1 during incubation of NQO1 with ES936 and NADH. Experimental data from LC/MS analysis demonstrated an increase in mass of 217 Da. Alkylation by an ES936-derived reactive iminium species would result in a theoretical increase

of mass of 218 Da, and this is within the errors of the multiple determinations that were performed. Since the data were consistent with this mechanism, we proceeded to attempt to identify the specific residues alkylated in the active site of hNQO1. LC/MS/MS analysis of a tetrapeptide detected after chymotryptic digestion of adducted and nonadducted hNQO1 demonstrated unequivocally that either Tyr 127 or Tyr 129 could be alkylated by the reactive iminium species. In agreement with the mechanism-based nature of the inhibition, either Tyr 127 or Tyr 129 was adducted but not both. We did not observe alkylation of the catalytic residue His 162 (*27*) by mass spectrometry. We cannot discount alkylation of this residue by the reactive iminium ion derived from ES936, but it was not detected in our analysis. It is possible that the instability of this adduct during MS analysis and the relatively high stability of the carbocation fragment ($m/z = 218$) precluded detection of this ion. Nevertheless, it is clear that alkylation of nucleophilic residues in the active site of hNQO1 occurs and satisfies another important criterion of mechanism-based inhibition (*43*).

Interestingly, the orientation of ES936 in the active site is reversed relative to that of the substrates EO9 and ARH019. The substrates bind in the active site with the 4,7-dione immersed in the catalytic pocket while ES936 binds in the opposite direction (*31*). While it is possible that this remains a characteristic of effective inhibitors, quinones which bind in this orientation are not necessarily inhibitors of NQO1. ES1340, an analogue of ES936 without a *p*-nitro group on the phenyl substituent of the indole ring, is not an inhibitor of hNQO1, but it binds to the active site of hNQO1 in an analogous orientation to ES936. This also demonstrates that the nitro substituent is not critical in determining the binding mode of ES936 in the active site. The different modes of binding of substrates such as EO9 and inhibitors such as ES936 within the same structural series make modeling interactions of quinones with hNQO1 difficult, and caution should be exercised in interpreting such studies. The binding of either ES936 or ES1340 to NQO1 buries between 618 Å^2 (ES1340) and 590 Å^2 (ES936) of apolar accessible area of the protein (total buried area between 734 and 778 Å^2). Burying the large water-accessible apolar area is more favorable from a thermodynamic perspective and is likely to drive the characteristic binding of such compounds.

Assessment of the involvement of NQO1 in complex metabolic systems has been hindered by the lack of specific inhibitors. Dicoumarol suffers from a number of problems including a lack of specificity, extensive protein binding, and its competitive, rather than irreversible, mechanism of action. In this paper, we have characterized ES936 as a potent mechanism-based inhibitor of hNQO1 which can be used as an additional indicator of the role of NQO1 in biological systems. Although ES936 is a mechanism-based inhibitor, no small molecule is likely to be totally specific for a particular enzyme. Since ES936 is also a quinone, caution should be exercised in its routine use as an NQO1 inhibitor until its effects in cellular systems have been carefully studied.

ACKNOWLEDGMENT

We thank Dr. Dan Gustafson for helpful discussions.

REFERENCES

1. Ernster, L. (1967) *Methods Enzymol. 10*, 309−317.
2. Lind, C., Hochstein, P., and Ernster, L. (1982) *Arch. Biochem. Biophys. 216*, 178−185.
3. Thor, H., Smith, M. T., Hartzell, P., Bellomo, G., Jewell, S. A., and Orrenius, S. (1982) *J. Biol. Chem. 257*, 12419−12425.
4. Beyer, R. E., Segura-Aguilar, J., Di Bernardo, S., Cavazzoni, M., Fato, R., Fiorentini, D., Galli, M., Setti, M., Landi, L., and Lenaz, G. (1996) *Proc. Natl. Acad. Sci. U.S.A. 93*, 2528−2532.
5. Landi, L., Fiorentini, D., Galli, M. C., Segura-Aguilar, J., and Beyer, R. E. (1997) *Free Radical Biol. Med. 22*, 329−335.
6. Siegel, D., Bolton, E. M., Burr, J. A., Liebler, D. C., and Ross, D. (1997) *Mol. Pharmacol. 52*, 300−305.
7. Huggins, C., and Fukunishi, R. (1964) *J. Exp. Med. 119*, 923−942.
8. Benson, A. M., Hunkler, M. J., and Talalay, P. (1980) *Proc. Natl. Acad. Sci. U.S.A. 77*, 5216−5220.
9. Talalay, P., De Long, M. J., and Prochaska, H. J. (1988) *Proc. Natl. Acad. Sci. U.S.A. 85*, 8261−8265.
10. Ross, D., Siegel, D., Beall, H., Prakash, A. S., Mulcahy, R. T., and Gibson, N. W. (1993) *Cancer Metastasis Rev. 12*, 83−101.
11. Ross, D., Beall, H., Traver, R. D., Siegel, D., Phillips, R. M., and Gibson, N. W. (1994) *Oncol. Res. 6*, 493−500.
12. Winski, S., Hargreaves, R. H. J., Butler, J., and Ross, D. (1998) *Clin. Cancer Res. 4*, 3083−3088.
13. Schlager, J. J., and Powis, G. (1990) *Int. J. Cancer 45*, 403−409.
14. Malkinson, A. M., Siegel, D., Forrest, G. L., Gazdar, A. F., Oie, H. K., Chan, D. C., Bunn, P. A., Mabry, M., Dykes, D. J., Harrison, S. D., Jr., and Ross, D. (1992) *Cancer Res. 52*, 4752−4757.
15. Siegel, D., Franklin, W. A., and Ross, D. (1998) *Clin. Cancer Res. 4*, 3083−3088.
16. Schelonka, L. P., Siegel, D., Wilson, M. W., Meininger, A., and Ross, D. (2000) *Invest. Ophthalmol. Visual Sci. 41*, 1617−1622.
17. Hollander, P., and Ernster, L. (1975) *Arch. Biochem. Biophys. 169*, 560−567.
18. Hosoda, S., Nakamura, W., and Hayashi, K. (1974) *J. Biol. Chem. 549*, 6416−6423.
19. Hulse, M., Feldman, S., and Bruckner, J. V. (1981) *J. Pharmacol. Exp. Ther. 218*, 416−420.
20. Preusch, P. C., Siegel, D., Gibson, N. W., and Ross, D. (1991) *Free Radical Biol. Med. 11*, 77−80.
21. Phillips, R. M. (1999) *Biochem. Pharmacol. 58*, 303−310.
22. Walton, M. I., Smith, P. J., and Workman, P. (1991) *Cancer Commun. 3*, 199−206.
23. Bailey, S. M., Suggett, N., Walton, M. I., and Workman, P. (1992) *Int. J. Radiat. Oncol. Biol. Phys. 22*, 649−653.
24. Beall, H. D., Hudnott, A. R., Winski, S., Siegel, D., Swann, E., Ross, D., and Moody, C. J. (1998) *Bioorg. Med. Chem. Lett. 8*, 545−548.
25. Beall, H. D., Winski, S., Swann, E., Hudnott, A. R., Cotterill, A. S., O'Sullivan, N., Green, S. J., Bien, R., Siegel, D., Ross, D., and Moody, C. J. (1998) *J. Med. Chem. 41*, 4755−4766.
26. Phillips, R. M., Naylor, M. A., Jaffar, M., Doughty, S. W., Everett, S. A., Breen, A. G., Choudry, G. A., and Stratford, I. J. (1999) *J. Med. Chem. 42*, 4071−4080.
27. Li, R., Bianchet, M. A., Talalay, P., and Amzel, L. M. (1995) *Proc. Natl. Acad. Sci. U.S.A. 92*, 8846−8850.
28. Faig, M., Bianchet, M. A., Talalay, P., Chen, S., Winski, S., Ross, D., and Mario, A. L. (2000) *Proc. Natl. Acad. Sci. U.S.A. 97*, 3177−3182.
29. Chen, S., Knox, R., Wu, K., Deng, P. S. K., Zhou, D. J., Bianchet, M. A., and Amzel, L. M. (1997) *J. Biol. Chem. 272*, 1437−1439.
30. Skelly, J. V., Sanderson, M. R., Suter, D. A., Baumann, U., Read, M. A., Gregory, D. S., Bennett, M., Hobbs, S. M., and Neidle, S. (1999) *J. Med. Chem. 42*, 4325−4330.
31. Faig, M., Bianchet, M. A., Winski, S., Hargreaves, R. H., Moody, C. J., Ross, D., and Amzel, L. M. (2001) *Structure* 9, 659−667.

32. Beall, H. D., Mulcahy, R. T., Siegel, D., Traver, R. D., Gibson, N. W., and Ross, D. (1994) *Cancer Res. 54*, 3196−3201.
33. Moody, C. J., and Swann, E. (1997) *Farmaco 52*, 271−279.
34. Otwinowski, Z., and Minor, W. (1996) *Methods Enzymol.*, 276.
35. Allen, F. H., and Kennard, O. (1993) *Chem. Des. Automation News 8*, 31−37.
36. Brunger, A. T., Adams, P. D., Clore, G. M., DeLano, W. L., Gros, P., Grosse-Kunstleve, R. W., Jiang, J. S., Kuszewski, J., Nilges, M., Pannu, N. S., Read, R. J., Rice, L. M., Simonson, T., and Warren, G. L. (1998) *Acta Crystallogr., Sect. D: Biol. Crystallogr. 54*, 905−921.
37. Jones, T. A., Zou, J. Y., Cowan, S. W., and Kjeldgaard (1991) *Acta Crystallogr. A47*, 110−119.
38. Kraulis, P. (1991) *J. Appl. Crystallogr. 24*, 946−950.
39. Esnouf, R. M. (1997) *J. Mol. Graphics Modell. 15*, 132−133.
40. Merrit E. A., and Bacon (1997) *Methods Enzymol. 277*, 505−524.
41. Nicholls, A., Sharp, K. A., and Honig, B. (1991) *Proteins 11*, 281−296.
42. Hubbard, S. A. T. J. (1993) *NACCESS Computer Program*, Department of Biochemistry and Molecular Biology, University College, London.
43. Silverman, R. B. (1988) *Mechanism based enzyme inactivation: Chemistry and Enzymology*, Vol. 1, CRC Press Inc., Boca Raton, FL.

BI011324I